Available online at www.sciencedirect.com
ScienceDirect
Carbohydrate Polymers 73 (2008) 371–377
Carbohydrate Polymers
www.elsevier.com/locate/carbpol

Isolation, preparation and characterization of cellulose microfibers obtained from bagasse

Deepanjan Bhattacharya [a,1], Louis T. Germinario [b], William T. Winter [c,*]

[a] Eastman Chemical Company, Global Coatings Application Development, Kingsport, TN 37662, USA
[b] Eastman Chemical Company, Kingsport, TN 37662, USA
[c] Cellulose Research Institute and Department of Chemistry, State University of New York College of Environmental Science and Forestry, 121 Edwin C. Jahn Laboratory, Syracuse, NY 13219, USA

Received 25 June 2007; received in revised form 1 December 2007; accepted 3 December 2007
Available online 15 December 2007

Abstract

Cellulose microfibers were isolated from bagasse in three distinct stages. Initially bagasse was subjected to a conventional pulping process to eliminate lignin and hemicellulose. Whole cellulosic fibers thus obtained were then mechanically separated into their constituent microfibrils (MFs) by a two-stage homogenization process and finally acid hydrolyzed. The dimensions of the resulting micro fibers were dependent on the hydrolysis conditions. Persistent discoloration indicated that cellulose obtained from bagasse, a sugarcane by-product, was far more resistant to hydrolysis than tunicate, bacterial, or even wood celluloses. Scanning Electron Microscopy (SEM) and Atomic Force Microscopy (AFM) indicated that the transverse size of the particles varied between 200 nm to a few microns. Solid-state NMR was also used to study the morphological changes taking place in cellulose as a result of the hydrolysis. A future goal is to use these MFs as reinforcing elements in composites with biodegradable thermoplastic co-polyesters or other common engineering thermoplastics, and this will be discussed in a subsequent report.

Keywords: Bagasse; Cellulose microfibers; Hydrolysis

1. Introduction

The use of very small asymmetric particles as reinforcement for high performance composites and other structural materials has attracted a great deal of interest. Most of the attention so far has focused on inorganic sources like clay (Vaia, Ishii, & Giannelis, 1993). In the last decade efforts have been directed towards obtaining such 'nano fillers' from other natural resources. Cellulose is the most abundant naturally occurring polymer on earth, and has emerged as a very strong candidate for providing such 'nanoparticles' as a reinforcing agent (Helbert, Cavaille, & Dufresne, 1996). The inherent stiffness and high degree of crystallinity make it ideally suited for reinforcing and load bearing applications in composites. Apart from this, cellulose is a sustainable resource, biodegradable in nature, inexpensive and has a much lower density than most fillers that are in use today.

Bagasse is the by-product obtained after sucrose extraction from the sugar cane plant. It has a high proportion of cellulose, which can be readily isolated from the other components namely lignin and hemicellulose, by pulping. Bagasse provides an ideal opportunity for producing value-added products from such an inexpensive source of biomass. Bagasse is also a by-product of the Brazilian sugar cane to bioethanol program where it is burned in cogeneration facilities (Zanin et al., 2000). It could equally well be used, in part, as a source of cellulose nanoparticles.

Controlled acid hydrolysis of native cellulose fibers disrupts the fibers which can then be dispersed into their constituent rod-shaped elementary crystalline microfibrils. Colloidal suspensions of these rods are known to exhibit birefringence and ordered liquid crystalline phases (Araki,

* Corresponding author. Tel.: +1 315 470 6876; fax: +1 315 470 6856.
E-mail addresses: dbhattacharya@eastman.com (D. Bhattacharya), germ@eastman.com (L.T. Germinario), cellulose@esf.edu (W.T. Winter).
[1] Tel.: +1 423 229 5016; fax: +1 423 224 9277.

0144-8617/$ - see front matter © 2008 Published by Elsevier Ltd.
doi:10.1016/j.carbpol.2007.12.005

Wada, Kuga, & Okano, 2000; Dong, Revol, & Gray, 1998; Marchessault, Morehead, & Walter, 1959; Orts, Godbout, Marchessault, & Revol, 1998; Revol et al., 1994). Cellulose from certain plant sources like *Valonia* spp. (Sassi & Chanzy, 1995) and animal sources like tunicates (Favier, Chanzy, & Cavaille, 1995) have already been reported to yield whisker like particles, the lateral dimensions of which are typically in the 3–20 nm range. Thus while the particles are commonly referred to as microfibers (MFs), they are, in fact, nanoparticulate in scale.

One of the goals in our laboratory has been to evaluate the use of certain sources of cellulose to produce '*nano-whiskers*' and incorporate them as a reinforcing component in biodegradable thermoplastic co-polyesters.

There has been no reported work on the use of bagasse as a source of producing highly crystalline MFs. The present study was conducted to demonstrate the possibility of isolating MFs from bagasse for future use as a nanoscale reinforcing filler. Scanning Electron Microscopy (SEM), Atomic Force Microscopy (AFM) as well as solid-state NMR spectroscopy was used to characterize the MFs and study the morphological changes taking place during the conversion process.

2. Experimental

2.1. Materials

The United States Sugar Corporation provided a 5 kg sample of bagasse. Sodium hydroxide and glacial acetic acid, for the initial pulping process were purchased from MCB and EM Science, respectively. Sulfuric acid was purchased from Fisher Scientific. All the chemicals were reagent grade or higher in purity and were used as received.

2.2. Purification of cellulose from bagasse

Oven dried bagasse was initially milled in a Wiley Mill to pass through a 40 mesh screen. Although bagasse composition reports are variable, one recent review suggests approximately 50% cellulose, 25% lignin and 25% hemicellulose (Pandey, Soccol, Nigam, & Soccol, 2000). Initially, the dried bagasse was digested at 80 °C in a 4% sodium hydroxide solution for 4 h. This removed the greater part of lignin and a large part of hemi cellulose. Because of persistent discoloration the product was subsequently bleached with a sodium chlorite/glacial acetic acid mixture to remove any residual lignin and hemi cellulose that may have been present. The bleached cellulose fibers were washed repeatedly, initially with a 5% aqueous sodium hydroxide and subsequently deionized water in order to attain a neutral pH.

2.3. Preparation of dispersed cellulose microfibers

A 5% suspension (w/w) of the cellulose fibers in water was warmed to 75 °C and then blended in a Cuisinart Vari-Speed blender for 10 min.

It was then homogenized in order to break down the fibers into smaller particles. Homogenization was carried out in a two-stage homogenization pump (APV Gaulin) at a pressure of 8000 psi (550 atm).

The APV Gaulin homogenizer consists of a reciprocating plunger which forces the suspension of the MFs through two small orifices at very high velocities. The extent of mechanical breakdown of the fibers can be controlled by regulating the pressure and additional recycling stages. Cellulose, thus obtained, was acid hydrolyzed by refluxing with 60% (w/v) sulfuric acid for 2.5 h at 60 °C to preferentially remove the non-crystalline regions, leaving a collection of well-dispersed micro fibers (Sassi & Chanzy, 1995). The reaction was quenched by the addition of ice water. The MFs were washed with water and dispersed for 5 min with repeated cooling using a Branson 450 sonifier. The dispersion medium was then gradually changed from water to tertiary butanol. The MFs were then freeze-dried from a suspension in *t*-butanol.

3. Methods

3.1. Microscopic techniques

Both Scanning Electron Microscopy (SEM) and Atomic Force Microscopy (AFM) were used to analyze the effect of hydrolysis and mechanical shearing on the supramolecular structure of cellulose.

After dispersion of cellulose fibrils in an ultrasonic bath, cellulose fragments were deposited on a glass slide and examined under a Zeiss Universal Microscope in order to assess the degree of dispersion. A drop of the aqueous suspension containing the acid treated microfibers was deposited on a polished graphite stub for structural analysis using a LEO, DSM 982, field emission scanning electron microscope (FEGSEM).

In order to accurately characterize surface topography and microfibril structure, all surface imaging was obtained using a commercial atomic force microscope (AFM), Dimension series D3000 AFM (Digital Instruments, Santa Barbara, CA). AFM was also used to observe surface morphology and crystalline orientation. Atomic force microscopy (AFM) using tapping mode is more suitable than contact mode for imaging polymer surfaces since the AFM tip intermittently contacts the surface leading to a minimization of destructive lateral forces that can produce surface artifacts. Therefore all AFM images were recorded in tapping mode.

3.2. Solid-state NMR studies

The extensive hydrogen bonding in the supramolecular structure of cellulose minimizes its solubility in most common NMR solvents. Hence, one has to resort taking NMR spectra of cellulose using a solid-state probe.

Solid-state Cross Polarization/Magic Angle Spinning (CP/MAS) ^{13}C NMR measurements were obtained at

75.01 MHz using a Bruker Avance 300 MHz spectrometer. Dry samples of cellulose (pre- and post-hydrolysis) were packed in 7 mm zirconia rotors and the measurements were performed using a CP pulse program with 1 ms match time and a 5 s delay between transients. Spinning rate was 5.0 ± 0.1 KHz. Calibration was done externally to the carbonyl carbon of glycine at 176 ppm.

4. Results and discussion

4.1. Scanning Electron Microscopy (SEM)

A definite change in the morphological structure of the whole cellulose fibers occurred upon acid hydrolysis and was observed using SEM. Fig. 1 is an optical micrograph of the cellulose fibers prior to hydrolysis. Typically most of the particles were 2 mm in length.

However, the SEM micrographs of the fibers post-hydrolysis indicated that majority of the microfibrils were in the sub-micron range having high, i.e. 50–120, aspect ratios. The larger bundles from which the microfibers were released after hydrolysis, ultrasonication and homogenization, can be seen in Fig. 2.

A broad distribution of fiber lateral dimensions is evident, owing to the fact that some of the microfibrillar bundles were still not completely dispersed and/or re-aggregated during the preparation of samples for SEM and AFM studies. Depending on their origin, cellulose microfibrils may have transverse dimensions that range from 20 to 200 nm but these particles are often aggregates, and the individual microfibrils are usually in the range of 3–20 nm (Sassi, 1995). Compared to the cellulose whiskers obtained from other sources like ramie (Frey-Wyssling, 1954), cotton (Frey-Wyssling, 1954), filter paper (Araki et al., 2000; Dong et al., 1998) or bleached kraft wood pulp (Revol, Bradford, Giasson, Marchessault, & Gray, 1992), the microfibril dimensions isolated from bagasse appeared to be less uniform. The aggregation phenomena of the individual microfibrils into fiber bundles were also less pronounced in certain other sources such as *Cladphora* (Hayashi, Sugiyama, Okano, & Ishihara, 1998) cellulose and *Valonia* (Sassi & Chanzy, 1995) cellulose under similar hydrolysis conditions. A distribution in the dimensions of the cellulose whiskers has also been reported previously.

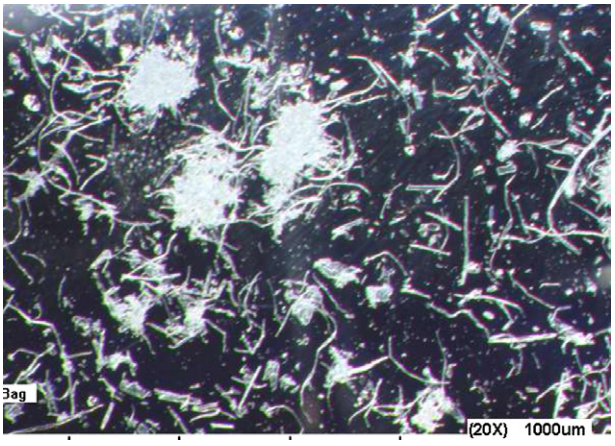

Fig. 1. Optical micrograph of whole cellulose fibers isolated from bagasse after pulping.

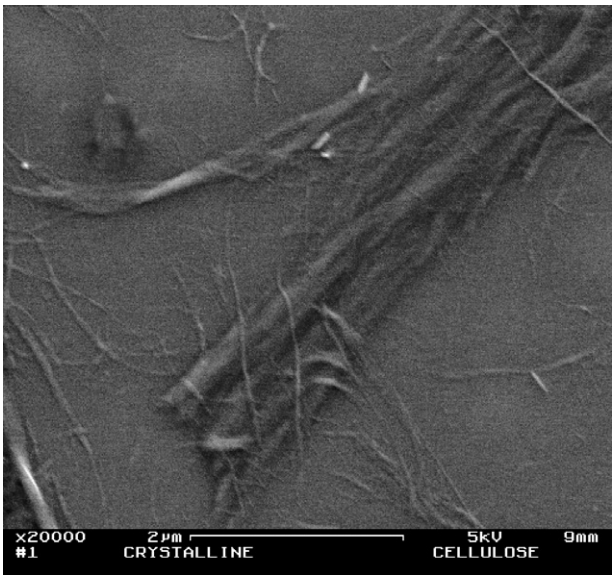

Fig. 2. Scanning Electron Micrograph showing the presence of the individual cellulose microfibers obtained from bagasse.

4.2. Atomic Force Microscopy (AFM)

There have been some recent reports on the crystal structure of cellulose using AFM. Baker, Helbert, Sugiyama, and Miles (2000) have used it to study the crystalline order in the bulk as well as on the surface for microcrystalline cellulose isolated from *Valonia Ventricosa*.

Images generated from our studies using the Atomic Force Microscopy illustrated the fiber bundle morphology in cellulose MFs isolated from bagasse.

In Fig. 3, we see the whole microfibrillar bundles, as well as, individual nanofibers. In this figure, the left-hand image is a height image that represents surface topography, while the right-hand image is a phase image whose contrast differentiates soft and hard polymer segments. Both height and phase images are recorded.

These images agree well with the scanning electron micrographs. Increased magnification of microfibrillar bundles reveals nanometer-scale (30 nm) structures (Fig. 4). These dimensions are comparable to those proposed by Hess et al., for their schematic representation of cellulose fiber structure (Hess, Kiessig, & Gundermann, 1941). The banding apparent in these images (Fig. 5), is consistent with the density fluctuations in the Hess model for the microfibrillar assembly. The presence of periods from 60 to 100 nm is representative of crystalline (bright regions) and amorphous (dark) regions in the direction of the fiber axis. For semi crystalline polymers, lighter areas in phase images have been interpreted as crystalline

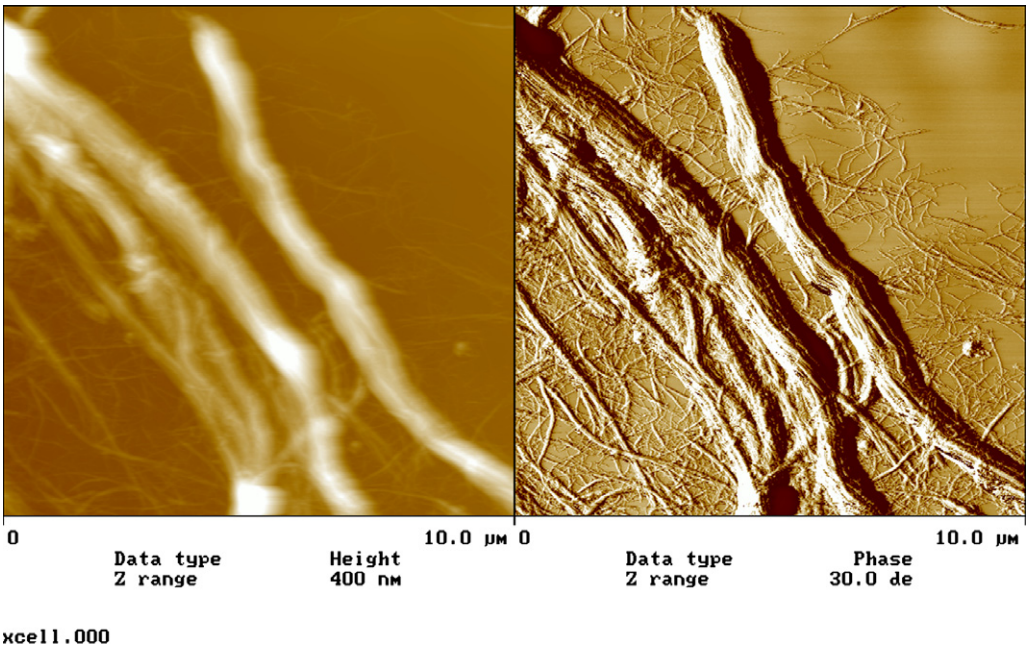

Fig. 3. AFM images showing the fiber bundle morphology in cellulose isolated from bagasse.

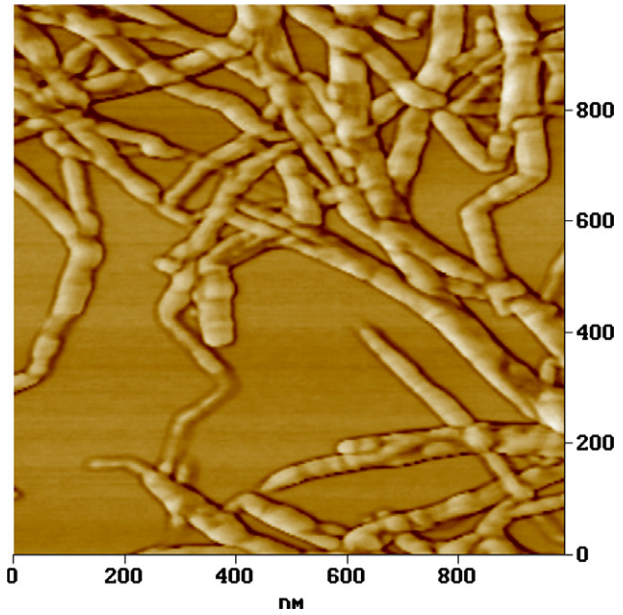

Fig. 4. Microfibrillar bundles are also observed to be composed of nanometer-sized (~30 nm) nanofibers.

domains, while darker regions are considered to be amorphous (Boyd & Badyal, 1997). Although the banding is longer than that described in the original Hess model, it is consistent with numerous reports of a leveling off degree of polymerization, LODP, for cellulose of approximately 150–200 glucose residues (Håkansson & Per Ahlgren, 2005). In a crystalline domain, each glucose residue subtends 0.5 nm along the major axis so a LODP of 150–200 nm corresponds to a crystallite length of 75–100 nm, as seen in Fig. 5.

4.3. Solid-state NMR studies

Cross Polarization/Magic Angle Spinning (CP/MAS) studies proved to be a very useful technique in monitoring the morphological changes taking place in cellulose during the course of hydrolysis. The ^{13}C NMR spectra of (a) intact cellulose fibers and (b) hydrolyzed MFs are presented in Fig. 6a and b, respectively. The six carbon atoms that are assigned to the cellulose molecule dominate the spectrum in both the cases. The chemical shift values range from 105 to 60 ppm. The anomeric carbon (C1) appears furthest downfield at around 105 ppm. This is followed by the signal from the C4 atom between 82 and 89 ppm. Peaks arising due to C2, C3 and C5 atoms make their appearance between 72 and 79 ppm and finally the C6 peak has a chemical shift value of 64 ppm.

The absence of any aromatic signals between 110 and 140 ppm clearly indicated that the lignin component present in bagasse had been successfully eliminated as a result of the alkali treatment and the subsequent bleaching process.

The earliest published work on the solid-state NMR spectra of cellulose showed two peaks in the chemical shift range 80–92 ppm and these have been assigned to the C4 carbon atom (Atalla, Gast, Sindorf, Bartuska, & Maciel, 1980; Earl & vanderHart, 1981). A relatively sharp peak was assigned to crystalline regions, and a relatively broad peak was attributed to the crystallite surfaces and the amorphous/disordered domains.

Previous assignments by Newman (Newman, 1998; Newman & Hemmingson, 1995). Horii, Hirai, and Kitamaru (1984) and Wickholm, Larsson, and Iversen (1998)

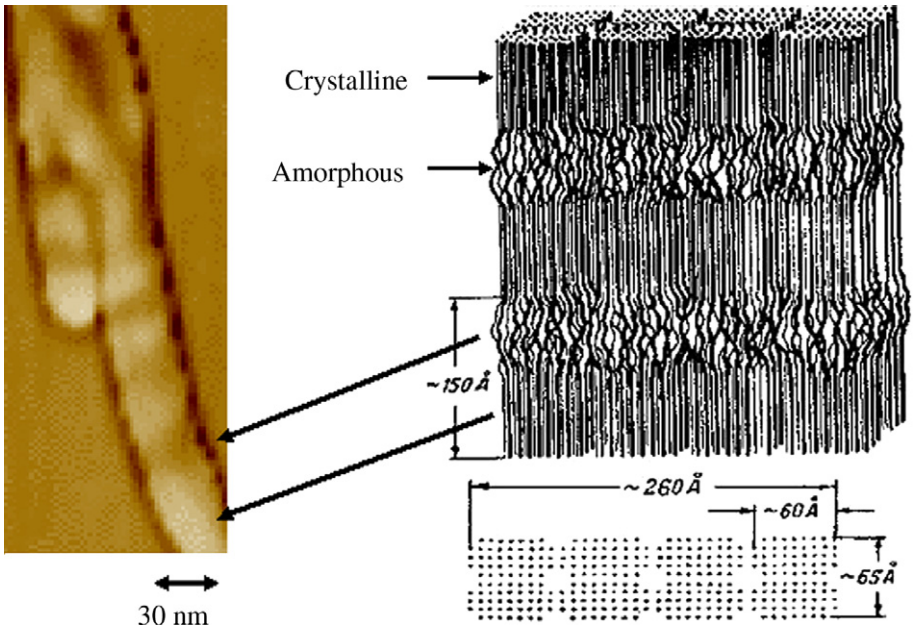

Fig. 5. AFM phase images support Hess et al. model for the presence of periods from 10 to 20 nm for the presence of crystalline and amorphous regions in the direction of the fiber axis.

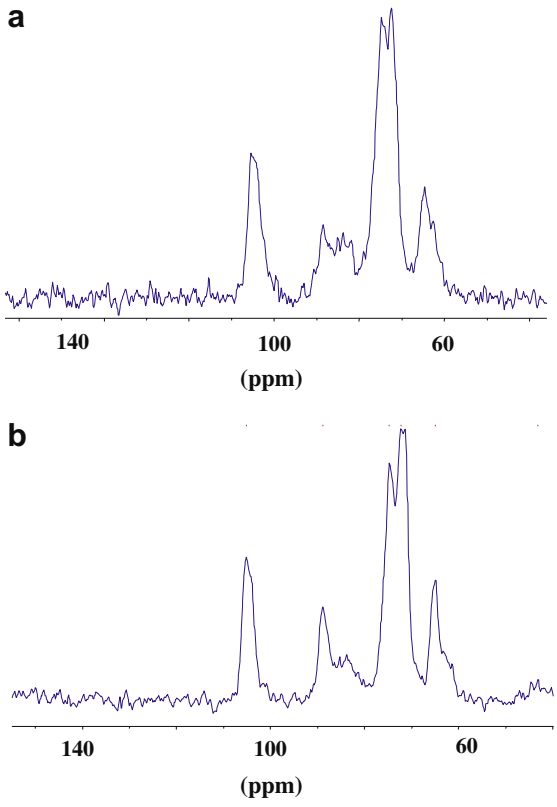

Fig. 6. (a) ^{13}C CP/MAS NMR spectra of cellulose fiber (whole cells). (b) ^{13}C CP/MAS spectra of cellulose microfibers after hydrolysis.

also helped in correlating the cellulose NMR spectra to structure and morphology. A slight shoulder on the C6 peak, between 63 and 65 ppm, has been attributed to the amorphous and disordered component in cellulose.

The ^{13}C NMR spectrum of the cellulose fibers before and after hydrolysis had some very distinct differences:

(i) The signal assigned to the C4 peak changed dramatically. There was a significant difference between the peak profiles of the crystalline and the amorphous components attributed to signals in this region (80–92 ppm) before and after hydrolysis and mechanical shearing. The unhydrolysed cellulose fibers exhibited roughly equal contributions from the crystalline and the amorphous domains (Fig. 7a).

Newman and his co-workers have made specific assignments to the signals arising from crystallite interiors, crystallite surfaces as well as the amorphous regions. Not such attempt was made in our case because of the problems associated with the signal to noise ratio. However after hydrolysis of the cellulose fibers, we find that the signal attributed to the crystalline regions at around 89 ppm is sharper and far better defined (Fig. 7b). Moreover, the ratio of the peak intensities between the crystalline and the amorphous regions also increases significantly. This observation agrees with our model of cellulose hydrolysis in which the accessible amorphous and surface regions react before the crystalline interiors. Thus, the increase in intensity (as well as sharpness) of the C4 crystalline component peak clearly indicates that we were successfully able to eliminate the amorphous and disordered domains leaving behind collections of well-defined crystalline microfibrils.

(ii) The C6 signal appearing at 63 ppm had a well-defined shoulder that has normally been attributed to the amorphous component in cellulose. We find that the hydrolytic treatment of the whole cellulose fibers resulted in the main C6 peak becoming sharper. The shoulder in the C6 signal that was associated with the disordered regions also decreased considerably. This provides further

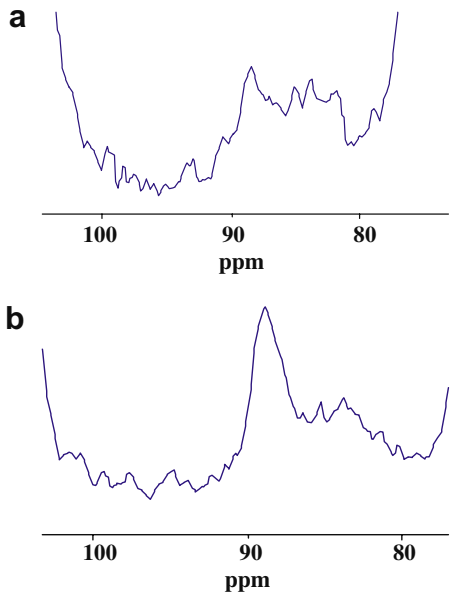

Fig. 7. Enlarged ^{13}C CP/MAS spectra of (a) whole cellulose fibers and (b) cellulose MFs obtained after hydrolysis.

support for preferential degradation of cellulose as a result of hydrolysis and mechanical dispersion.

5. Conclusions

We were successfully able to isolate cellulose fibers from bagasse. Mechanical shearing and controlled hydrolysis were required to separate the whole cellulose fibers into micron-sized particles. Hydrolysis of the cellulose fibers with 60% (w/v) sulfuric acid for 2.5 h at 60 °C was found to be optimum since it resulted in the removal of most of the amorphous domains without any significant damage to the crystal structure. There was a distribution in the size of the MFs and it ranged from a few 100 nm to a couple of microns. Total release of all the individual MFs from the microfibrillar bundles was not possible under the above mentioned hydrolysis dispersion conditions. More drastic conditions did lower the aggregation phenomena between the individual MF, but at the same time it also resulted in extensive crystal damage.

Solid-state NMR spectroscopy of the cellulose fibers did confirm that all the lignin had been eliminated during the pulping process. The ^{13}C NMR spectra of the MFs also clearly indicated that hydrolysis and mechanical shearing resulted in significant removal of the amorphous regions that were initially present in the unhydrolysed cellulose fibers.

References

Araki, J., Wada, M., Kuga, S., & Okano, T. (2000). Birefringent glassy phase of a cellulose microcrystal suspension. *Langmuir, 16*(6), 2413–2415.

Atalla, R. H., Gast, J. C., Sindorf, D. W., Bartuska, V. J., & Maciel, G. E. (1980). Carbon-13 NMR spectra of cellulose polymorphs. *Journal of the American Chemical Society, 102*(9), 3249–3251.

Baker, A. A., Helbert, W., Sugiyama, J., & Miles, M. J. (2000). New insight into cellulose structure by atomic force microscopy shows the I (crystal phase at near-atomic resolution. *Biophysical Journal, 79*(2), 1139–1145.

Boyd, R. D., & Badyal, J. P. S. (1997). Nonequilibrium plasma treatment of miscible polystyrene/poly(phenylene oxide) blends. *Macromolecules, 30*(18), 5437–5442.

Dong, X. M., Revol, J. F., & Gray, D. G. (1998). Effect of microcrystallite preparation conditions on the formation of colloid crystals of cellulose. *Cellulose, 5*(1), 19–32.

Earl, W. L., & VanderHart, D. L. (1981). Observations by high-resolution carbon-13 nuclear magnetic resonance of cellulose I related to morphology and crystal structure. *Macromolecules, 14*(3), 570–574.

Favier, V., Chanzy, H., & Cavaille, J. Y. (1995). Polymer nanocomposites reinforced by cellulose whiskers. *Macromolecules, 28*(18), 6365–6367.

Frey-Wyssling, A. (1954). The fine structure of cellulose microfibrils. *Science, 119*, 80–82.

Håkansson, H., & Per Ahlgren, P. (2005). Acid hydrolysis of some industrial pulps: Effect of hydrolysis conditions and raw material. *Cellulose, 12*(2), 177–183.

Hayashi, N., Sugiyama, J., Okano, T., & Ishihara, M. (1998). Selective degradation of the cellulose Ia component in Cladophora cellulose with Trichoderma viride cellulase. *Carbohydrate Research, 305*(1), 109–116.

Helbert, W., Cavaille, J. Y., & Dufresne, A. (1996). Thermoplastic nanocomposites filled with wheat straw cellulose whiskers: Part I. Processing and mechanical behavior. *Polymer Composites, 17*(4), 604–611.

Hess, K., Kiessig, H., & Gundermann, J. (1941). X-ray and electron-microscopic investigations of the process of grinding of cellulose. *Zeitschrift fur physik. Chemie, B49*, 64–82.

Horii, F., Hirai, A., & Kitamaru, R. (1984). CP/MAS carbon-13 NMR study of spin relaxation phenomena of cellulose containing crystalline and noncrystalline components. *Journal of Carbohydrate Chemistry, 3*(4), 641–662.

Marchessault, R. H., Morehead, F. F., & Walter, N. M. (1959). Liquid crystal systems from fibrillar polysaccharides. *Nature, 184*(9), 632–633.

Newman, R. H., & Hemmingson, J. A. (1995). Carbon-13 NMR distinction between categories of molecular order and disorder in cellulose. *Cellulose, 2*(2), 95–110.

Newman, R. H. (1998). Evidence for assignment of ^{13}C NMR signals to cellulose crystallite surfaces in wood, pulp, and isolated celluloses. *Holzforschung, 52*(2), 157–159.

Orts, W. J., Godbout, L., Marchessault, R. H., & Revol, J.-F. (1998). Enhanced ordering of liquid crystalline suspensions of cellulose microfibrils: A small-angle neutron scattering study. *Macromolecules, 31*(17), 5717–5725.

Pandey, A., Soccol, C. R., Nigam, P., & Soccol, V. T. (2000). Biotechnological potential of agro-industrial residues I: Sugarcane bagasse. *Bioresource Technology, 74*(1), 69–80.

Revol, J.-F., Bradford, H., Giasson, J., Marchessault, R. H., & Gray, D. G. (1992). Helicoidal self-ordering of cellulose microfibrils in aqueous suspension. *International Journal of Biological Macromolecules, 14*(3), 170–172.

Revol, J. F., Godbout, L., Dong, X. M., Gray, D. G., Chanzy, H., & Maret, G. (1994). Chiral nematic suspensions of cellulose crystallites; phase separation and magnetic field orientation. *Liquid Crystals, 16*(1), 127–134.

Sassi, J. -F. (1995). Etude ultrastructurale de l'acetylation de la cellulose application à la preparation de nanocomposites, Doctoral Thesis, Univ. Joseph Fourier, Grenoble, France.

Sassi, J. F., & Chanzy, H. (1995). Ultrastructural aspects of the acetylation of cellulose. *Cellulose, 2*(2), 111–127.

Vaia, R. A., Ishii, H., & Giannelis, E. P. (1993). Synthesis and properties of two-dimensional nanostructures by direct intercalation of polymer melts in layered silicates. *Chemistry of Materials, 5*(12), 1694–1696.

Wickholm, K., Larsson, P. T., & Iversen, T. (1998). Assignment of non-crystalline forms in cellulose I by CP/MAS carbon-13 NMR spectroscopy. *Carbohydrate Research, 312*(3), 123–129.

Zanin, G. M., Santana, C. C., Bon, E. P. S., Giordano, R. C. L., de Moraes, F. F., Andrietta, S. R., et al. (2000). Brazilian bioethanol program. *Applied Biochemistry and Biotechnology, 84–86*(1–9), 1147–1161.